
**PROTEIN CHEMISTRY AND
STRUCTURE:**

**Tetratricopeptide Repeat (TPR) Motifs of
p67 *phox* Participate in Interaction with
the Small GTPase Rac and Activation of
the Phagocyte NADPH Oxidase**

Hirofumi Koga, Hiroaki Terasawa, Hiroyuki
Nunoi, Koichiro Takeshige, Fuyuhiko Inagaki
and Hideki Sumimoto

J. Biol. Chem. 1999, 274:25051-25060.

doi: 10.1074/jbc.274.35.25051

Access the most updated version of this article at <http://www.jbc.org/content/274/35/25051>

Find articles, minireviews, Reflections and Classics on similar topics on the [JBC Affinity Sites](#).

Alerts:

- [When this article is cited](#)
- [When a correction for this article is posted](#)

[Click here](#) to choose from all of JBC's e-mail alerts

This article cites 58 references, 33 of which can be accessed free at
<http://www.jbc.org/content/274/35/25051.full.html#ref-list-1>

Tetratricopeptide Repeat (TPR) Motifs of p67^{phox} Participate in Interaction with the Small GTPase Rac and Activation of the Phagocyte NADPH Oxidase*

(Received for publication, March 5, 1999, and in revised form, May 11, 1999)

Hirofumi Koga‡§, Hiroaki Terasawa¶||, Hiroyuki Nunoi**, Koichiro Takeshige§, Fuyuhiko Inagaki¶||, and Hideki Sumimoto‡§ ‡‡

From the ‡Department of Molecular and Structural Biology, Kyushu University Graduate School of Medical Science, 3-1-1 Maidashi, Higashi-ku, Fukuoka 812-8582, Japan, the §Department of Biochemistry, Kyushu University School of Medicine, Fukuoka 812-8582, Japan, the ¶Department of Molecular Physiology, Tokyo Metropolitan Institute of Medical Science, Tokyo 113-8613, Japan, ||CREST, Japan Science and Technology Corporation (JST), and the **Department of Pediatrics, Kumamoto University School of Medicine, Kumamoto 860-8556, Japan

The small GTPase Rac functions as a molecular switch in several important cellular events including cytoskeletal reorganization and activation of the phagocyte NADPH oxidase, the latter of which leads to production of superoxide, a precursor of microbicidal oxidants. During formation of the active oxidase complex at the membrane, the GTP-bound Rac appears to interact with the N-terminal region of p67^{phox}, another indispensable activator that translocates from the cytosol upon phagocyte stimulation. Here we show that the p67^{phox} N terminus lacks the CRIB motif, a well known Rac target, but contains four tetratricopeptide repeat (TPR) motifs with highly α -helical structure. Disruption of any of the N-terminal three TPRs, but the last one, results in defective interaction with Rac, while all the four are required for the NADPH oxidase activation. We also find that Arg-102 in the third repeat is likely involved in binding to Rac via an ionic interaction, and that replacement of this residue with Glu completely abrogates the capability of activating the oxidase both *in vivo* and *in vitro*. Thus the TPR motifs of p67^{phox} are packed to function as a Rac target, thereby playing a crucial role in the active oxidase complex formation.

Rac1 and Rac2, members of the Rho family of small GTPases, play a pivotal role in several important cellular functions including cytoskeletal reorganization, gene expression, and activation of the phagocyte NADPH oxidase following microbial infection (1, 2). Rac serves as a molecular switch cycling between an active GTP-bound and an inactive GDP-bound states. In the active state, Rac interacts with a variety of target (effector) proteins to elicit cellular responses (1, 2). For example, the protein kinase PAK is activated by interacting with Rac in a GTP-dependent manner (3). This interaction is mediated via binding of Rac to a Cdc42/Rac interactive binding (CRIB)¹

* This work was supported in part by grants from the Ministry of Education, Science, Sports, and Culture of Japan, the Uehara Memorial Foundation, the Kato Memorial Bioscience Foundation, the Fukuoka Cancer Society, and CREST (Core Research for Evolutional Science and Technology) of Japan Science and Technology Corp. (JST). The costs of publication of this article were defrayed in part by the payment of page charges. This article must therefore be hereby marked "advertisement" in accordance with 18 U.S.C. Section 1734 solely to indicate this fact.

‡‡ To whom correspondence should be addressed: Dept. of Molecular and Structural Biology, Kyushu University Graduate School of Medical Science, 3-1-1 Maidashi, Higashi-ku, Fukuoka 812-8582, Japan. Tel.: 81-92-642-6213; Fax: 81-92-642-6215; E-mail: hsumi@mailserver.med.kyushu-u.ac.jp.

¹ The abbreviations used are: CRIB, Cdc42/Rac interactive binding;

motif within the N-terminal regulatory region of PAK, a motif that is present in a variety of targets of Rac and Cdc42 (4). Although more than 10 targets of Rac have been discovered (1), molecular natures of the interactions, except the CRIB motif, remain largely unknown. It is thus considered important to study Rac-target interactions especially in functionally well defined systems.

The phagocyte NADPH oxidase, dormant in resting cells, is activated during phagocytosis to produce superoxide, a precursor of microbicidal oxidants (5–8). The significance of the enzyme in host defense is indicated by chronic granulomatous disease (CGD) patients suffering from recurrent severe infection caused by defect of the superoxide producing activity (7, 8). Although the NADPH oxidase is originally discovered in phagocytes because of its abundance, it has recently been proposed that the enzyme is expressed in a variety of cells and reactive oxygen species derived from superoxide that play a role in several signal transduction systems (6). The redox core of the oxidase is a membrane-spanning flavocytochrome, cytochrome *b*₅₅₈, comprising the two subunits gp91^{phox} and p22^{phox}. Upon cell stimulation three cytosolic proteins, namely p47^{phox}, p67^{phox}, and Rac, translocate to membranes, where they interact with the cytochrome to form an active oxidase complex. All the five polypeptides are required for activation of the NADPH oxidase *in vitro*, and CGD is caused by defect of any of the genes encoding these proteins except Rac (5–8).

In assembly and activation of the phagocyte NADPH oxidase, protein-protein interactions between the oxidase factors play a crucial role (5, 9, 10). Both p47^{phox} and p67^{phox} harbor two SH3 domains, which mediate specific interactions between the factors: the C-terminal SH3 domain of p67^{phox} interacts with p47^{phox}, while the N-terminal one of p47^{phox} does with p22^{phox} (11–15). At least two events elicited during intracellular signal transduction in stimulated cells appear to function as a switch of the oxidase activation. One of the two is a conformational change of p47^{phox}: the N-terminal SH3 domain of p47^{phox} is normally inaccessible, and, upon cell stimulation, becomes unmasked to interact with p22^{phox}, an induced interaction that is required for the oxidase activation (12, 15, 16).

The other critical event seems to be conversion of Rac to the active state: only the GTP-bound Rac, but not the GDP-bound one, activates the oxidase under cell-free conditions (16–19), and introduction of Rac antisense oligonucleotides or expres-

CGD, chronic granulomatous disease; TPR, tetratricopeptide repeat; CD, circular dichroism; GST, glutathione *S*-transferase; PAGE, polyacrylamide gel electrophoresis; PMA, phorbol 12-myristate 13-acetate; GTP γ S, guanosine 5'-3-*O*-(thio)-triphosphate.

sion of a dominant negative form of Rac2 (T17N) inhibits superoxide production in stimulated cells (20, 21). Rac1 in the GTP-bound state can directly interact with the N-terminal region of p67^{phox}, comprising approximately 200 amino acid residues (22). This region lacks a CRIB motif, an established target of Rac (4), but appears to contain tetratricopeptide repeat (TPR) motifs, as suggested solely by sequence alignment with other proteins containing the motif (23, 24). Since Rac proteins with a mutation leading to defective interaction with p67^{phox} are unable to activate the oxidase (22, 25–27), the interaction is considered to be involved in the oxidase activation. The final conclusion that Rac-p67^{phox} interaction is required, however, has awaited studies using mutant proteins of the target p67^{phox}.

Here we demonstrate that the p67^{phox} N-terminal region of about 200 residues is not only sufficient but also required for fully interacting with Rac. Circular dichroism (CD) spectrum of the region reveals that it contains highly α -helical structure, and comparison between human and mouse p67^{phox} supports the idea that the required region contains four TPR motifs, the first three of which are tandemly arranged. TPR motifs, each comprising a pair of antiparallel α -helices (24), are initially identified as a tandemly repeated degenerate 34-amino acid sequence in the nuclear protein Nuc2p (28) and the cell cycle division genes *cdc16*, *cdc13*, and *cdc27* (29, 30). It is now realized that the motif occurs in a wide variety of proteins present in organisms as diverse as bacteria, archaea, and eukarya (31, 32), and is involved in protein-protein and protein-lipid interactions (33, 34). Little is, however, known about molecular nature of TPR-mediated interactions.

Based on the crystal structure of the TPRs of the protein phosphatase PP5 (24), we have introduced mutations that are expected either to disrupt or to unaffected packing of the TPR helices of p67^{phox}. The present findings show that the N-terminal three TPRs, but the last one, are packed to interact with Rac, and that Arg-102 in the third TPR is likely involved in binding to Rac via an ionic interaction. The results obtained here also provide evidence that the interaction between p67^{phox} and Rac is required for the NADPH oxidase activation both *in vivo* and *in vitro*. Although the fourth TPR is dispensable for the interaction, it appears to play an essential role in the oxidase activation.

EXPERIMENTAL PROCEDURES

Preparation of cDNAs of Mutant Rac2 and p67^{phox}—The DNA fragments encoding various forms of human Rac2 were constructed by polymerase chain reaction-mediated mutagenesis, all of which contained the C189S substitution to avoid being modified by isoprenylation (35). Constitutively active and dominant negative forms of Rac2 carried the Q61L and T17N substitutions, respectively. Mutations in the effector loop (D38K and D38R substitutions) were introduced into the active Rac2 to obtain Rac2 (D38K/Q61L) and Rac2 (D38R/Q61L). The DNA fragments encoding mutant forms of p67^{phox} were also constructed by polymerase chain reaction-mediated site-directed mutagenesis. All the constructs were sequenced to confirm their identity.

Interaction between Rac and p67^{phox} in the Yeast Two-hybrid System—In the yeast two-hybrid system to investigate interaction between Rac and p67^{phox}, we used yeast strains HF7c containing two GAL4-inducible reporter genes, *HIS3* and *lacZ*. The multiple cloning sites of pGBT9 (CLONTECH), containing the GAL4 DNA-binding domain, and pGADGH (CLONTECH), containing the GAL4 *trans* activation domain, were modified so that the inserts from glutathione S-transferase (GST) fusion protein plasmids pGEX-2T (Pharmacia) can be readily transferred in correct orientation and reading frames, to obtain pGBT9g and pGADGHg (14). Yeast cells were co-transfected with pairs of two-hybrid plasmids and selected by growth on medium lacking tryptophan and leucine. Cells containing both plasmids were picked up and plated on a histidine-lacking medium to test protein-protein interaction.

Overlay Assay to Detect Interactions between Purified Recombinant Proteins—The DNA fragment encoding a constitutively active form of Rac2 (Q61L) was subcloned into the (His)₆-tagged fusion protein plas-

mid pProEX-HTb expression vector (Life Technologies, Inc.). The DNA fragments encoding p67^{phox} and its mutants were subcloned into the pGEX-2T expression vector (Amersham Pharmacia Biotech). (His)₆-tagged or GST fusion proteins were expressed in the *Escherichia coli* strain BL21DE3 (Novagen) and purified by His-bind resin (Novagen) or glutathione-Sepharose 4B beads (Amersham Pharmacia Biotech), respectively, according to the manufacturer's protocol.

Various p67^{phox} fused to GST (10 μ g) were transferred to a nitrocellulose filter using Hybri-slot (Life Technologies, Inc.) according to the manufacturer's protocol. The filter was incubated with the blocking buffer (3% bovine serum albumin, 0.1% Triton X-100, 0.5 mM MgCl₂, 5 mM dithiothreitol) for 2 h, and washed two times with buffer A (50 mM Tris, pH 7.5, 100 mM NaCl, 5 mM MgCl₂, 0.1 mM dithiothreitol). His-tagged Rac2 (Q61L/C189S) (0.2 μ g) was preloaded for 30 min at 30 °C with 2 μ l of [γ -³²P]GTP (NEN Life Science Products Inc; 6000 Ci/mmol, 10 mCi/ml, 0.8 M) in the GTP-loading buffer (50 mM Tris-HCl pH 7.5, 5 mM EDTA, 0.5 mg/ml bovine serum albumin). The freshly prepared probe was incubated for 5 min at room temperature with the GST fusion proteins on the filter in buffer A containing 1 mM GTP and 1 mg/ml bovine serum albumin. The filter was washed 3 times with an ice-cold washing buffer (20 mM Tris, pH 7.5, 150 mM NaCl, and 0.1% Tween 20). After the filter was dried up, it was exposed to a Fuji Imaging plate (Fuji Photo Co.), and signals were detected with the image scanner STORM (Molecular Dynamics).

Cell-free Activation of the Phagocyte NADPH Oxidase—The membrane fraction of human neutrophils was prepared as described previously (12). The DNA fragment encoding p47^{phox} was subcloned into the (His)₆-tagged fusion protein plasmid pET-28a(+) expression vector (Novagen). The fusion proteins were expressed in *E. coli* strain BL21DE3 (Novagen) and purified by His-bind resin (Novagen), according to the manufacturer's protocol. The neutrophil membrane (17.5 μ g/ml) was mixed with His-tagged Rac2 (7.5 μ g/ml) preloaded with 100 μ M GTP γ S, His-tagged p47^{phox} (3.7 μ g/ml), and the indicated concentration of GST-p67^{phox} or its mutants, followed by incubation with an optimal concentration of SDS (100 μ M) for 2.5 min at room temperature in potassium phosphate buffer (100 mM, pH 7.0) containing 75 μ M cytochrome *c*, 10 μ M FAD, 1.0 mM EGTA, 1.0 mM MgCl₂, and 1.0 mM NaN₃. The reaction was initiated by addition of NADPH (250 μ M) to the reaction mixture. The production of superoxide was measured at the rate of superoxide dismutase-inhibitable ferricytochrome *c* reduction at 550–540 nm with a dual-wavelength spectrophotometer (Hitachi 557) (15, 16).

Transfection of Wild-type and R102E Mutant p67^{phox} in gp91^{phox} and p47^{phox}-transduced K562 Cells—We used a retroviral vector system, pSXLc/pHa, that utilizes an internal ribosome entry site fragment of encephalomyocarditis virus (36), to transduce the gp91^{phox} gene into the leukemia cell line K562 that expresses p22^{phox} but not gp91^{phox} (37). Cells highly expressing gp91^{phox} were selected using FACS scan with the monoclonal antibody 7D5 to detect functional cytochrome *b*₅₅₈ comprising the two subunits gp91^{phox} and p22^{phox} (38). A bicistronic retrovirus vector encoding a human multidrug resistance gene (*MDR1*) and the p47^{phox} gene (pHa-MDR-IRES-p47) (39) were further transduced to the stably transduced gp91^{phox}-expressing K562 cells. The doubly transduced cells were selected with 4 ng/ml vincristine, expanded in a drug-free medium, and used for the following experiments.

Complementary DNAs encoding the full-length of wild-type and mutant p67^{phox} carrying the R102E substitution were subcloned into pREP10 (Invitrogen), which were transfected by electroporation to the K562 cells that stably express both gp91^{phox} and p47^{phox}. The K562 cells (2×10^7 cells/ml) were electroporated in the presence of 10 μ g of the wild-type or mutant form of p67^{phox} plasmid DNA at 170 V, 960 microfarads using Gene Pulser (Bio-Rad). At 48 h post-transfection, cells were selected for 5 days with 250 μ g/ml hygromycin B.

Expression of Oxidase Factors in K562 Cells—For detection of p47^{phox} and p22^{phox}, K562 cells were sonicated and the lysates were applied to 10% SDS-polyacrylamide gel electrophoresis (PAGE). Proteins were transferred to a polyvinylidene difluoride membrane (Millipore), and probed with polyclonal antibodies raised against the C-terminal peptide of p47^{phox} and with an anti-p22^{phox} monoclonal antibody.

For detection of p67^{phox}, proteins were immunoprecipitated from the K562 cell lysates (2×10^7 cells) with rabbit polyclonal antibodies raised against the C-terminal peptide of p67^{phox} and protein A-Sepharose (Pharmacia). After incubation for 3 h at 4 °C, the beads were washed four times with ice-cold phosphate-buffered saline (137 mM NaCl, 2.7 mM KCl, 4.3 mM Na₂HPO₄, and 1.4 mM KH₂PO₄, pH 7.0). Bound proteins were resuspended in the SDS sample buffer, subjected to SDS-PAGE (10%), and transferred to a polyvinylidene difluoride membrane (Millipore). The membrane was probed with an anti-p67^{phox} monoclonal antibody (12).

Activation of the NADPH Oxidase in the Whole Cell System—Superoxide production by the K562 cells expressing wild-type or mutant p67^{phox} was determined as superoxide dismutase-inhibitable chemiluminescence detected with an enhancer-containing luminol-based detection system (DIOGENES; National Diagnostics) as described by de Mendez *et al.* (37).

After the selection, K562 cells (2×10^6 cells) were resuspended in 1 ml of HBSS buffer (17 mM HEPES, pH 7.4, 120 mM NaCl, 5 mM KCl, 5 mM glucose, 1 mM MgCl₂, and 1 mM CaCl₂). After the addition of the enhanced luminol-based substrate (40 μ l), the cells were stimulated for 30 min at 37 °C with 200 ng/ml phorbol 12-myristate 13-acetate (PMA). The chemiluminescence was assayed using luminometer (Auto Lumat LB953; EG & G Berthold). The reaction was stopped by the addition of superoxide dismutase (50 μ g/ml).

Circular Dichroism (CD) Spectra—GST-p67 (1–203) and GST-p67 (1–203, R102E) were expressed in the *E. coli* strain BL21DE3 (Novagen) and purified by glutathione-Sepharose 4B beads (Amersham Pharmacia Biotech), as described above. After thrombin digestion to remove the GST tag, the protein fragments, namely p67 (1–203) and p67 (1–203, R102E), were purified on a Q-Sepharose (Amersham Pharmacia Biotech) and RESOURSE S (Amersham Pharmacia Biotech), and their purities were analyzed by 12% SDS-PAGE. The concentrations of the proteins used for these studies were 5 μ M in 10 mM sodium phosphate, pH 6.4. CD measurements were performed with a Jasco J-725 spectrometer using rectangular quartz cells of 0.2-cm path length at 20 °C. Far-UV CD spectra were the average of eight accumulations taken at 50 nm/min. Secondary structural components were calculated by the method of Yang *et al.* (40) using software supplied by Jasco, Inc.

NMR Measurements—The proteins without tags, p67 (1–203) and p67 (1–203, R102E), were dissolved at concentrations of 1 mM in 50 mM sodium phosphate, 150 mM NaCl, and 10 mM dithiothreitol-*d*₁₀ in 90% H₂O and 10% D₂O, and then adjusted to pH of 6.9 (direct pH meter reading). Their ¹H NMR spectra were recorded on a UNITY inova 500 spectrometer operating at ¹H 500 MHz and 25 °C with a spectral width of 7000 Hz. Chemical shifts were referenced relative to the internal standard 2,2-dimethyl-2-silapentane-5-sulfonate.

RESULTS

The N-terminal Region of p67^{phox} Is Both Required and Sufficient for Interaction with Rac—To explore the region of p67^{phox} for binding to Rac2, we prepared a series of deletion mutants of p67^{phox} to use them for the yeast two-hybrid system. A constitutively active form of Rac2, carrying the Q61L substitution, interacted with the full-length p67^{phox} (p67-F) (Fig. 1A), which agrees with the result obtained by the yeast two-hybrid system using a different reporter system (35). Two C-terminal deleted p67^{phox}, p67-N (amino acids 1–242) and p67 (1–203), fully interacted with Rac2 (Fig. 1A). The findings indicate that the N-terminal region of p67^{phox} is sufficient for the interaction with Rac, which is consistent with the results obtained from an *in vitro* binding assay using purified proteins (22). On the other hand, a dominant negative form of Rac2, namely Rac2 (T17N), was incapable of interacting with p67-F, p67-N, or p67 (1–203) (Fig. 1B and data not shown), confirming that the GTP-bound Rac2, but not the GDP-bound one, binds to p67^{phox}. Further deletion of p67 (1–203) from either its N or C terminus resulted in complete loss of the interaction with Rac2 (Fig. 1A). These results suggest that the p67^{phox} N-terminal domain comprising about 200 residues is both required and sufficient for binding to Rac2.

When Rac1 was used instead of Rac2, the same results were obtained: GTP-bound Rac1 interacted with the N terminus of p67^{phox} (data not shown). These Rac GTPases share 92% amino acid identity with the identical effector loop of amino acid residues 32–40. Some mutations in the loop region result in impaired interaction with p67^{phox} (22, 27) as well as decreased ability to support the NADPH oxidase activation (22, 41). One such mutation is substitution of Asn, a neutral hydrophilic residue, for Asp-38 (27). Replacement of this residue by basic ones (D38K and D38R) also abrogated the interaction with p67^{phox} (Fig. 1B). These observations raise the possibility that Asp-38 may interact with a basic residue in the N terminus of

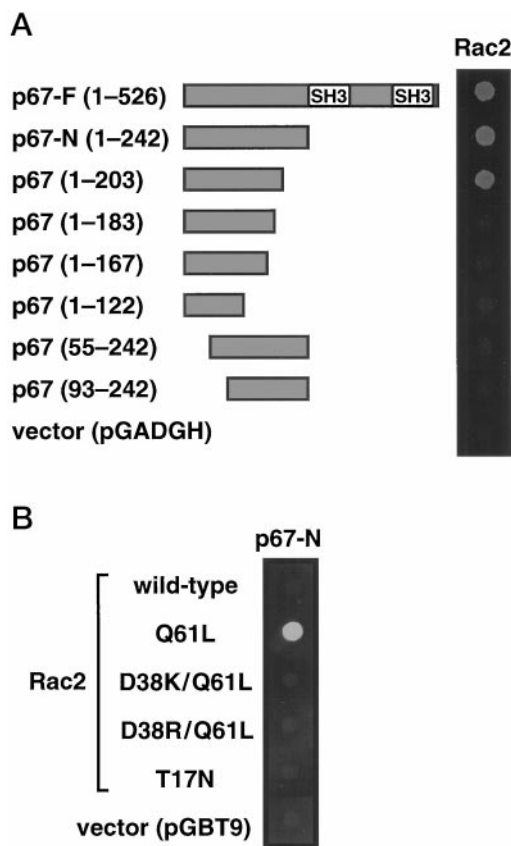


FIG. 1. Interaction between Rac2 and p67^{phox}. A, interaction of Rac2 with the N-terminal region of p67^{phox}. The yeast reporter strain HF7c was co-transfected with pairs of recombinant plasmids pGBT9 and pGADGH, the former encoding a constitutively active form of Rac2 (Rac2 (Q61L)) fused to the GAL4 DNA-binding domain, and the latter encoding various deletion mutants of p67^{phox} (numbers indicate amino acid residues from the first methionine) fused to the GAL4 transactivation domain. Its histidine-independent growth was tested as described under "Experimental Procedures." B, interaction of various Rac2 with the N-terminal region of p67^{phox}. The yeast reporter strain HF7c was co-transfected with recombinant plasmids pGBT9 encoding Rac2 carrying various mutations and pGADGH encoding p67-N (amino acid residues 1–242): Q61L, a constitutively active form of Rac2; D38K/Q61L and D38R/Q61L, proteins with additional D38K and D38R substitutions, respectively; and T17N, a dominant negative form. Its histidine-independent growth was tested as described under "Experimental Procedures."

p67^{phox}. To define residues of p67^{phox} involved in Rac binding, we substituted the neutral residue Gln for each of all eight Arg residues that occur in the p67^{phox} N terminus (Fig. 2A). The R102Q substitution resulted in severely impaired interaction with Rac2, while the R38Q or R77Q substitution led to a slight defect of the interaction (Fig. 2B). On the other hand, five other mutant proteins carrying an Arg \rightarrow Gln substitution at 62, 66, 155, 184, or 188 interacted with Rac2 as strongly as the wild-type one did (Fig. 2B).

Four TPR Motifs Occur in the Rac-binding Domain of p67^{phox}—The binding experiment using p67^{phox} proteins with substitution of Gln for Arg suggests that approximately 150 residues from the N terminus play a more important role, since the substitution at 155, 184, or 188 did not affect the interaction with Rac2 (Fig. 2). A search of SwissProt data base with this region by Blastp algorithm revealed a weak sequence similarity (20–30% identity) to regions of Ssn6p, a general transcriptional repressor in *Saccharomyces cerevisiae* (42), and also, to a lesser extent, those of human CDC27 protein (43) and yeast TOM70, the 70-kDa translocase of outer membrane in mitochondria (44). The regions of these proteins are composed

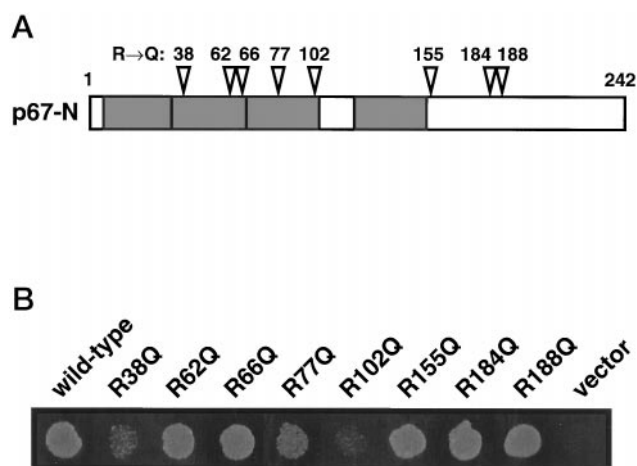


FIG. 2. Roles of Arg residues in interaction between Rac2 and p67^{phox}. *A*, schematic representation of the eight Arg residues in the N terminus of p67^{phox}. Arrowheads with the residue number indicate the position of the eight Arg residues contained in the N-terminal region of p67^{phox}. Each shaded box represents TPR motif. *B*, interaction of Rac2 with p67^{phox} carrying an Arg → Gln mutation. The yeast reporter strain HF7c was co-transfected with recombinant plasmids pGBT9 encoding Rac2 (Q61L) and pGADGH encoding p67^{phox} carrying an Arg → Gln mutation. Its histidine-independent growth was tested as described under “Experimental Procedures.”

of TPR motifs. The motif is a degenerate 34-amino acid sequence identified in a wide variety of proteins, present in tandem arrays of 3–16 motifs (24, 28, 29, 31). Although there exists no position characterized by an invariant residue, a consensus sequence pattern of small and large hydrophobic residues has been defined: small hydrophobic residues are commonly observed at positions 8, 20, and 27, while large ones are at 4, 17, and 24 (24, 31). Careful alignment of the N terminus of p67^{phox} suggests that the region comprises four copies of the TPR motif, although the first repeat contains only 31 residues (Fig. 3A), the possibility which is also pointed out by other investigators (23, 24). In all four motifs of p67^{phox}, there exist small hydrophobic residues at positions 8, 20, and 27, and large hydrophobic ones at 4, 17, and 24. In addition, like other TPR sequences, the N-terminal domain of p67^{phox} are quite hydrophilic as estimated from hydrophilicity/hydrophobicity plots (45).

Further support for the identity of the p67^{phox} N-terminal region as a TPR domain came from comparison between human p67^{phox} and its mouse homologue, the sequence of which we have recently determined (46). Since mouse p67^{phox} not only interacts with human Rac2 but also can replace human p67^{phox} in a cell-free activation system of human NADPH oxidase (46), critical residues of p67^{phox} are likely conserved between mouse and human. Alignment of amino acid sequences of human and mouse p67^{phox} revealed that most of substitutions in the TPRs occur at nonconsensus positions; consensus residues are selectively conserved between the two species (Fig. 3B).

To obtain direct information on the structure of the N terminus of p67^{phox} (residues 1–203) as a TPR domain, we isolated the fragment (Fig. 4A) and measured the circular dichroism (CD) spectrum (Fig. 4B). The profile, with the maximum at 190 nm and minima at 208 and 220 nm, is characteristic of an α -helix. The proportions of α -helix, β -sheet, and remaining structures were estimated by the method of Yang *et al.* (40) to be 76.3, 0, and 23.7%, respectively. This finding supports the idea that the N terminus of p67^{phox} contains TPR motifs, since the motif comprises a pair of antiparallel α -helices (24). Taken together, we concluded that the N-terminal region of p67^{phox} contains four TPR motifs, the first three being tandemly ar-

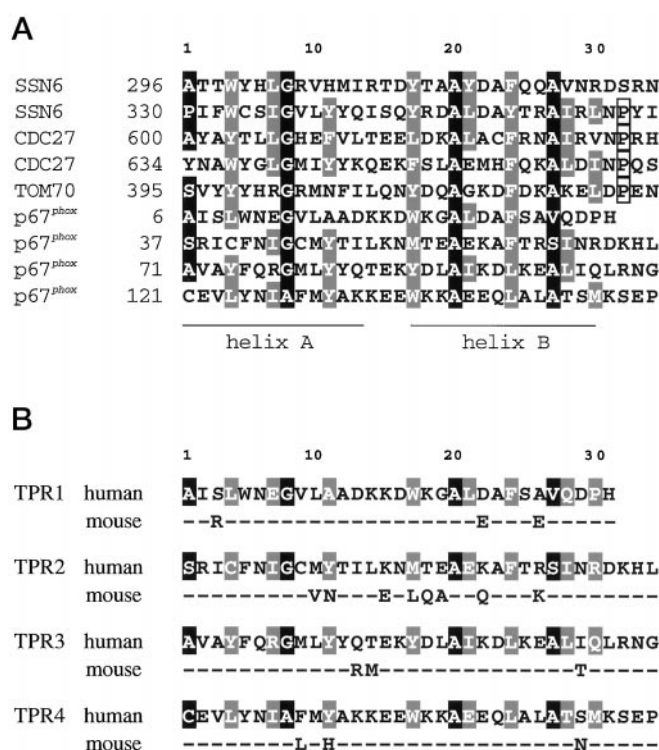


FIG. 3. TPR motifs in p67^{phox}. *A*, sequence alignment of the TPR motifs of SSN6, CDC27, TOM70, and p67^{phox}. Consensus TPR motif residues are shown with black and shaded boxes for small and large hydrophobic residues, respectively. Small hydrophobic residues are commonly observed at positions 8, 20, and 27. Position 32 is frequently proline (boxed), located at the C terminus of helix B, and large hydrophobic residues are also located at particular positions, especially 4, 17, and 24. *B*, the TPR motifs of human and mouse p67^{phox}. Indicated residues of mouse p67^{phox} (46) are different from those of human one. Consensus positions in the TPR motif are shown with black and shaded boxes for small and large hydrophobic residues, respectively.

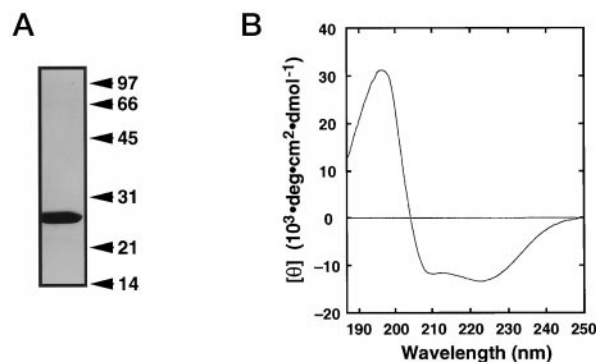


FIG. 4. Far-UV CD spectrum for the N-terminal region of p67^{phox} (p67 (1–203)). *A*, p67 (1–203) was purified and analyzed on SDS-PAGE, as described under “Experimental Procedures.” Positions of molecular size standards are indicated to the right in kilodaltons. *B*, the far-UV CD spectrum of p67 (1–203) (5 μ M) was measured at 20 °C in 10 mM sodium phosphate, pH 6.4.

ranged, while 16 extra residues are located between the third and fourth repeats (see Fig. 2A).

Role of p67^{phox} TPR Motifs in Binding to Rac—To clarify roles for each TPR motif of p67^{phox} in binding to Rac, we introduced two types of systematic mutations that are expected to disrupt each TPR architecture, based on the crystal structure of the TPR domain of the protein phosphatase PP5 (24). Each of the three TPR motifs of this domain consists of a pair of antiparallel α -helices of equivalent length, termed helix A and helix B (Fig. 3). Adjacent TPR motifs are packed together

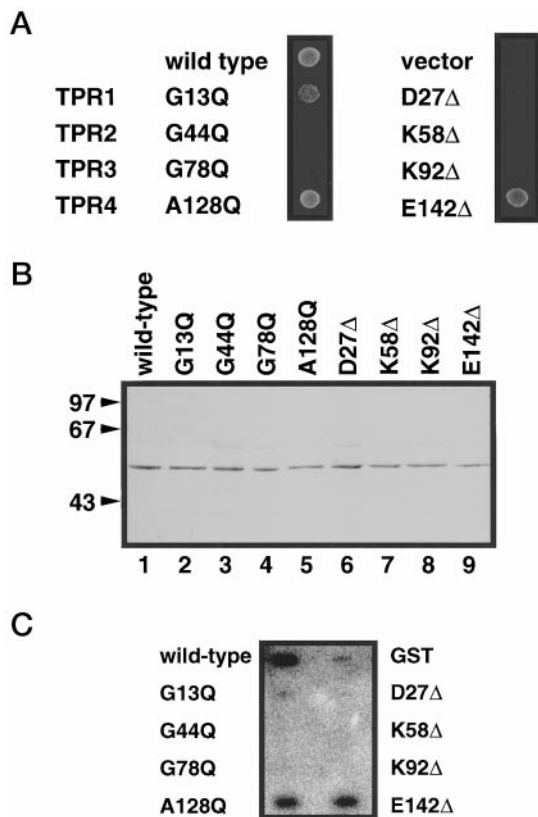


FIG. 5. Interaction of Rac2 with two types of TPR mutants of p67^{phox}. The first type of the mutations introduced into p67^{phox} (left) carries a substitution of the bulky residue Gln for a conserved small residue at position 8; G13Q, G44Q, G78Q, and A128Q. The second type (right) mutation is deletion of an amino acid residue at position 22 in the TPR motifs; D27Δ, K58Δ, K92Δ, and E142Δ. *A*, The yeast reporter strain HF7c was co-transfected with recombinant plasmids pGBT9 encoding Rac2 (Q61L) and pGADGH encoding various TPR mutants of p67^{phox}. Its histidine-independent growth was tested as described under "Experimental Procedures." *B*, SDS-PAGE analysis of wild-type and TPR mutants of p67^{phox}. Each sample (0.1 μg) as GST fusion protein is resolved on a 10% SDS-PAGE and visualized with Coomassie Brilliant Blue. Lane 1, GST-p67-N; lane 2, GST-p67-N (G13Q); lane 3, GST-p67-N (G44Q); lane 4, GST-p67-N (G78Q); lane 5, GST-p67-N (A128Q); lane 6, GST-p67-N (D27Δ); lane 7, GST-p67-N (K58Δ); lane 8, GST-p67-N (K92Δ); and lane 9, GST-p67-N (E142Δ). Positions of molecular size standards are indicated to the left in kilodaltons. *C*, analysis of Rac2 binding activity of various TPR mutants of p67^{phox} by an overlay assay. Each wild-type or mutant p67^{phox} (10 μg) as GST fusion protein were put on a nitrocellulose filter, and probed with His-tagged Rac2 preloaded with [³²P]GTP. The filter was exposed to an imaging plate, which was subjected to the image scanner, as described under "Experimental Procedures."

in a parallel arrangement such that a tandem TPR motif structure is composed of a regular series of antiparallel α -helices (24).

The first type of the mutations introduced into p67^{phox} is substitution of the bulky residue Gln for a conserved small residue at position 8 (Gly-13, Gly-44, Gly-78, or Ala-128). Such mutations are expected to cause the incorrect packing of neighboring helices of a TPR (Ref. 24, for detail, see "Discussion"), and a similar mutation at this position of the third TPR of p67^{phox} (G78E) has been reported to cause CGD (47). The substitution in the second or third TPR (G44Q or G78Q, respectively) led to severely impaired two-hybrid interaction with Rac2 (Fig. 5A). While the protein carrying the first TPR mutation (G13Q) weakly interacted with Rac2, the mutation in the last TPR (A128Q) did not affect the interaction (Fig. 5A). It is possible that these substitutions may destabilize the proteins, thereby resulting in a loss of two-hybrid interactions. To ex-

clude the possibility, we purified mutant proteins as GST fusions (Fig. 5B) and tested their ability to bind to Rac2 by an overlay assay. As shown in Fig. 5C, a negligible binding was observed using the proteins with a substitution in any of the N-terminal three TPRs, whereas GTP-bound Rac2 interacted well with the mutant p67^{phox} carrying the A128Q substitution. Thus the TPR motifs of p67^{phox}, except the last one, are likely involved in Rac interaction. Alternatively, one or more of the three TPRs may play a critical role in the correct overall folding of the TPR domain, which is required for binding to Rac2. Involvement of the second and third TPRs is also supported by the observation that the interaction with Rac2 is prevented by one amino acid substitution within helix A of these TPR (R38Q and R77Q) (Fig. 2).

For the second type of mutation, we deleted a residue at position 22 in the TPR motifs (Asp-27, Lys-58, Lys-92, and Glu-142). The deletion of position 22 is expected to change the spacing between the conserved small residues (positions 20 and 27) within helix B, leading to the incorrect packing between adjacent TPRs (Ref. 24; for detail see "Discussion"). One of the deletions, K58Δ, occurs in a patient with CGD, whose p67^{phox} is relatively unstable and defective in binding to Rac (48). Experiments using the yeast two-hybrid system showed that Rac binding activities of proteins with the first to third TPR motif mutation (D27Δ, K58Δ, and K92Δ) were severely reduced or abolished, while that of the fourth TPR mutant (E142Δ) was preserved as well as the wild-type protein (Fig. 5A). The *in vitro* binding activities by the overlay assay using the purified mutant proteins (Fig. 5B) were consistent with those obtained by the yeast two-hybrid system (Fig. 5C), confirming a crucial role of the first three TPRs.

All TPR Motifs of p67^{phox} Are Required for Activation of the NADPH Oxidase—The N terminus of p67^{phox}, p67 (1–242), is enough to fully activate the phagocyte NADPH oxidase in a cell-free system reconstituted with human neutrophil membrane, p47^{phox}, and Rac2 (16). To study the role of the TPR motifs of p67^{phox} in the oxidase activation, we prepared the protein lacking the first three or all TPR motifs, namely p67 (126–242) or p67 (170–242), respectively (Fig. 6A), and estimated their abilities to activate the enzyme in the cell-free system (15, 16). Both proteins were incapable of supporting superoxide production under the cell-free conditions, even at 2 order higher concentrations than those for p67 (1–242), containing all the four motifs, to activate the oxidase (less than 1 μg/ml) (Fig. 6B).

To estimate importance of each TPR motif, we next used the p67^{phox} proteins carrying a mutation in one of the TPRs (Fig. 5). The proteins with a mutation in the first three TPRs were unable to activate the NADPH oxidase (Fig. 6C). The incapability is likely due to that these mutant proteins are not able to interact with Rac2 (Fig. 5). Intriguingly, the proteins carrying the A128Q substitution or the deletion of Glu-142 showed little or no activity for the oxidase activation (Fig. 6C), although both mutant proteins fully interacted with Rac (Fig. 5). Thus the fourth TPR plays an essential role in activation of the NADPH oxidase, possibly interacting with other oxidase factors such as cytochrome *b*₅₅₈ or p47^{phox}.

Arg-102 in the Third TPR of p67^{phox} Is Involved in Rac Binding, Probably via an Ionic Interaction—As shown above (Fig. 2), the replacement of the basic residue Arg-102 by the neutral hydrophilic residue Gln resulted in severely defective interaction with Rac2. This residue, at position 32 of the third TPR of p67^{phox}, is conserved between mouse and human (Fig. 3B). The position is located at the C terminus of helix B, and thus is expected to be exposed but not involved in defining the TPR architecture, as in the TPR domain of PP5 (24). Therefore

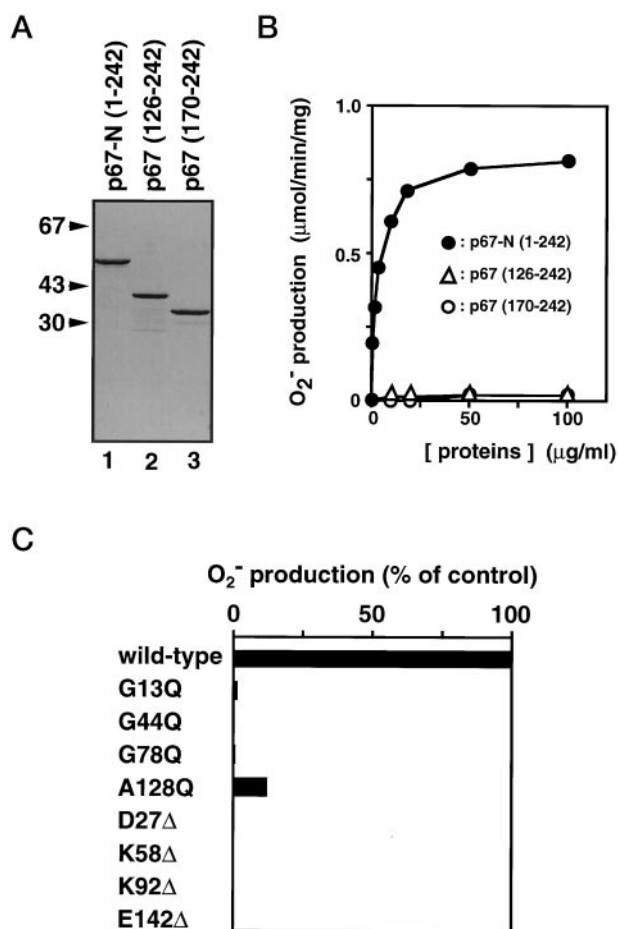


FIG. 6. Ability of various mutant p67^{phox} to activate the phagocyte NADPH oxidase under cell-free conditions. *A*, SDS-PAGE analysis of p67-N (1–242) and its deletion mutants. Each sample (0.5 μg) as GST fusion protein was resolved on a 12% SDS-PAGE and visualized with Coomassie Brilliant Blue. Lane 1, GST-p67-N (1–242); lane 2, GST-p67 (126–242); and lane 3, GST-p67 (170–242). Position of molecular size standards are indicated to the left in kilodaltons. *B*, human neutrophil NADPH oxidase was activated with the indicated concentration of the GST-p67-N or its deletion mutants, in the presence of His-tagged p47^{phox} (3.74 μg/ml), His-tagged Rac2 (7.3 μg/ml), and human neutrophil membranes (17.5 μg/ml). Filled circles, open triangles, and open circles indicate superoxide producing activities using p67-N (1–242), p67 (126–242), and p67 (170–242), respectively. Superoxide production was determined as described under “Experimental Procedures.” *C*, human neutrophil NADPH oxidase was activated with the wild-type or TPR mutants of GST-p67-N (10 μg/ml) under conditions as described in *B*.

it is possible that Arg-102 conforms a binding surface and a positive charge of this residue mediates the interaction with Rac. To test these possibilities, we introduced one amino acid substitution for Arg-102. The mutant p67^{phox} with the substitution of the positively charged residue Lys (R102K) could interact with Rac2, but to a lesser extent, as assessed by the yeast two hybrid-system (Fig. 7A) as well as by an overlay assay using purified proteins (Fig. 7, B and C). On the other hand, the replacement by the neutral residue Ala or Leu (R102A or R102L, respectively), like the R102Q substitution, led to a severely defective interaction with Rac (Fig. 7). The protein carrying the substitution of the acidic residue Glu (R102E) could not bind to Rac2 at all (Fig. 7).

To rule out the possibility that the R102E substitution results in a disrupted structure of the TPR domain, we measured both CD and ¹H NMR spectra of the protein with this mutation. The CD spectrum of the mutant protein (data not shown) was in complete agreement with that of the wild-type one (Fig. 4B):

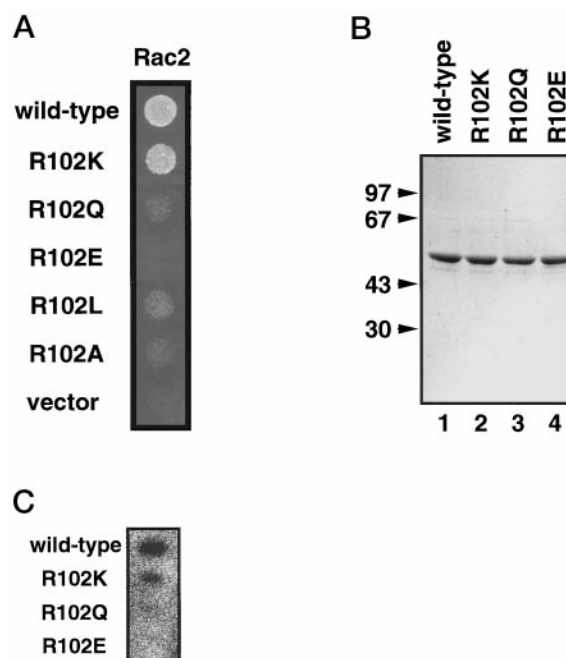


FIG. 7. Effects of substitutions for Arg-102 in p67^{phox} on binding to Rac2. *A*, Rac2 binding activities of p67^{phox} carrying various substitutions for Arg-102 were tested in the yeast two-hybrid system. The yeast reporter strain HF7c was co-transfected with recombinant plasmids pGBT9 encoding Rac2 (Q61L) and pGADGH encoding p67-N carrying various substitutions for Arg-102. Its histidine-independent growth was tested as described under “Experimental Procedures.” *B*, SDS-PAGE analysis of wild-type and various mutant forms of p67^{phox}. Each sample (0.4 μg) as GST fusion protein was resolved on a 10% SDS-PAGE and visualized with Coomassie Brilliant Blue. Lane 1, GST-p67-N; lane 2, GST-p67-N (R102K); lane 3, GST-p67-N (R102Q); and lane 4, GST-p67-N (R102E). Position of molecular size standards are indicated to the left in kilodaltons. *C*, analysis of Rac2 binding activity of mutant p67^{phox} carrying substitutions for Arg-102 by an overlay assay. The wild-type and mutant p67^{phox} as GST fusion proteins (10 μg) were put on a nitrocellulose filter, and probed with His-tagged Rac2 preloaded with [³²P]GTP. The filter was exposed to an imaging plate, which was subjected to the image scanner, as described under “Experimental Procedures.”

the estimated proportions of α-helix, β-sheet, and remaining structures in the mutated TPR domain were 76.9, 0, and 23.1%, respectively. We also tested the stability of the proteins by gradually increasing temperature from 20 to 60 °C: the changes in helical content were monitored at 222 nm. The curve for the changes of the R102E mutant protein was the same as that of the wild-type one (data not shown), supporting the idea that the α-helices of the p67^{phox} TPR domain are not disrupted by the substitution.

Furthermore, and most importantly, little difference could be observed between ¹H NMR spectra of the wild-type and R102E protein (Fig. 8), indicating that the mutated TPR domain is correctly folded. Thus the R102E substitution appears to unaffected the structural integrity of the protein. Taken together with the results obtained by the binding experiments, it is concluded that Arg-102 of p67^{phox} is involved in binding to Rac, probably via an ionic interaction.

Arg-102 Plays an Important Role in the Oxidase Activation In Vitro—To elucidate the role of Arg-102 in the NADPH oxidase activation, we tested the activity of mutant proteins carrying various substitutions for Arg-102 under the cell-free conditions. The protein with substitution of the basic residue Lys (R102K) was capable of supporting superoxide production, but to a lesser extent than the wild-type one (Fig. 9). Replacement by the neutral residue Gln (R102Q) or the acidic residue Glu (R102E) resulted in little or no activation of the NADPH oxi-

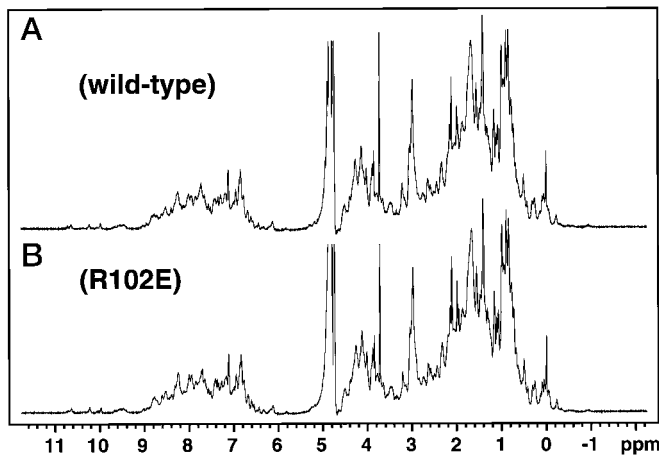


FIG. 8. Comparison of ^1H NMR spectra between p67 (1–203) and p67 (1–203, R102E). 500 MHz ^1H NMR spectra of p67 (1–203) (A) and p67 (1–203, R102E) (B) were measured in 50 mM sodium phosphate, 150 mM NaCl, and 10 mM dithiothreitol- d_{10} in 90% H_2O and 10% D_2O at 25 $^\circ\text{C}$ as described under “Experimental Procedures.”

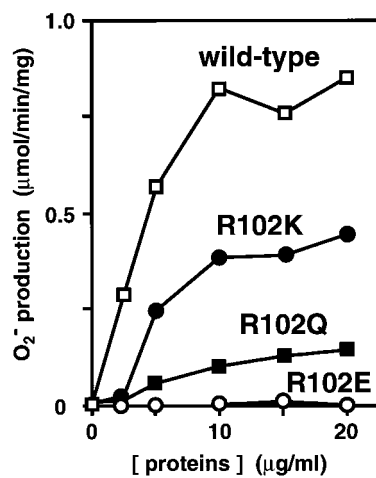


FIG. 9. Ability of various mutant p67^{phox} with substitution for Arg-102 to activate the phagocyte NADPH oxidase under cell-free conditions. Superoxide production was measured as described under “Experimental Procedures” using the indicated concentration of the wild-type or mutant GST-p67-N, His-tagged p47^{phox} (3.74 $\mu\text{g}/\text{ml}$), His-tagged Rac2 (7.3 $\mu\text{g}/\text{ml}$), and human neutrophil membranes (17.5 $\mu\text{g}/\text{ml}$). Open squares, filled circles, filled squares, and open circles indicate superoxide producing activities using p67-N (wild-type), p67-N (R102K), p67-N (R102Q), and p67-N (R102E), respectively.

dase, respectively (Fig. 9). The order of potency to activate the oxidase (the wild-type > R102K > R102Q > R102E) agrees with that to bind to Rac (Fig. 7), providing strong evidence that oxidase activation requires the interaction between p67^{phox} and Rac. Thus activation of the NADPH oxidase likely involves an ionic interaction with Rac via Arg-102 in the third TPR of p67^{phox}, which is consistent with that this TPR plays a crucial role in the activation (Fig. 6C).

p67^{phox} Carrying the R102E Substitution Is Incapable of Supporting the NADPH Oxidase Activation in a Whole Cell System—We finally investigated the role of Arg-102 in the NADPH oxidase activation *in vivo*, using a whole cell system of K562 cells, which is similar to the one that has been developed by Leto’s group (37). The cell line expresses Rac and low levels of endogenous p22^{phox}, but requires expression of the other three oxidase factors (gp91^{phox}, p47^{phox}, and p67^{phox}) to exhibit superoxide production in response to PMA (37). To explore the function of p67^{phox}, we transduced K562 cells for stable expression of gp91^{phox} and p47^{phox} using retroviral vectors encoding

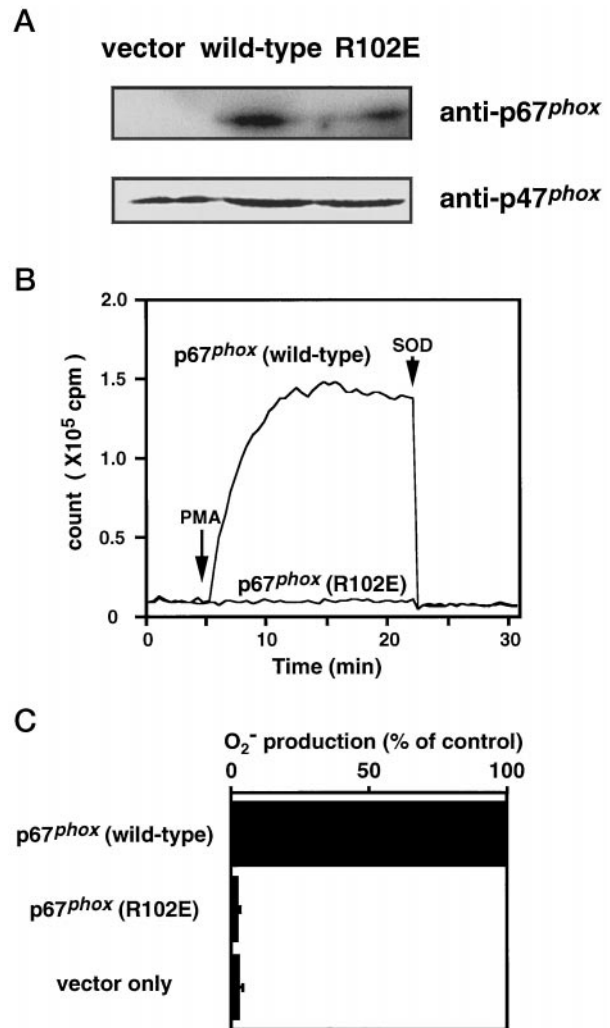


FIG. 10. Role of Arg-102 of p67^{phox} in the NADPH oxidase activation in a whole cell system. A, expression of p67^{phox} in gp91^{phox} and p47^{phox}-transduced K562 cells. The doubly transduced K562 cells were transfected with pREP10 vector or the vector to express the indicated form of p67^{phox}. In the upper panel, cell lysates were immunoprecipitated with rabbit anti-p67^{phox} polyclonal antibodies, and the samples were resolved by SDS-PAGE, transferred to a polyvinylidene difluoride membrane, and immunoblotted with a mouse anti-p67^{phox} monoclonal antibody. In the lower panel, cell lysates were immunoblotted with rabbit anti-p47^{phox} polyclonal antibodies. B, PMA-induced chemiluminescence by gp91^{phox} and p47^{phox}-transduced K562 cells transfected with the wild-type or R102E mutant of p67^{phox}. The K562 cells expressing the indicated form of p67^{phox} (2×10^6 cells/ml) were stimulated with PMA (200 ng/ml) and the chemiluminescence change was continuously monitored with an enhanced luminol-based substrate, DIOGENES. Superoxide dismutase (SOD) (50 $\mu\text{g}/\text{ml}$) was added where indicated. C, superoxide production by gp91^{phox} and p47^{phox}-transduced K562 cells transfected with the wild-type or R102E mutant of p67^{phox}. Superoxide production is expressed as the percent activity relative to control cells transfected with wild-type p67^{phox}. Each graph represents the mean of data from seven independent transfections, with bars representing the standard deviation of percent activity ($n = 7$).

the proteins. The transduced cells expressed functional cytochrome b₅₅₈ comprising the two subunits gp91^{phox} and p22^{phox} (data not shown; see “Experimental Procedures”) and p47^{phox} (Fig. 10).

The doubly transduced K562 cells were subsequently transfected with the episomal vector pREP10 that contained cDNA encoding the full-length wild-type p67^{phox} (p67-F) or full-length p67^{phox} with the R102E substitution, namely p67-F (R102E). The wild-type p67^{phox}-expressing cells fully produced superoxide when stimulated with PMA (Fig. 10). On the other hand,

the cells transfected with the p67-F (R102E) cDNA were unable to support superoxide production in response to PMA, although the protein was expressed at a similar level as the wild-type p67^{phox} in the control cells (Fig. 10). Thus the mutant p67^{phox} with the R102E substitution is incapable of activating the phagocyte NADPH oxidase under both cell-free and whole cell conditions.

DISCUSSION

Here we present that TPR motifs of p67^{phox} are involved in the interaction with the small GTPase Rac, both structurally and functionally. The binding to Rac requires an overall structure of the p67^{phox} N-terminal domain comprising about 200 amino acid residues in the proper conformation. The domain contains four TPR motifs, the N-terminal three being tandemly arranged, while 16 extra residues are located between the third and fourth TPRs. The present results show that the first three TPRs, but not the last one, play an essential role in the binding to Rac, via directly interacting with the GTPase and/or via being folded for the correct packing of the TPR domain. In particular, the third TPR appears to be directly involved in the interaction with Rac: Arg-102 in the third TPR, a residue that is likely irresponsible for the packing, participates in the interaction, probably via an ionic bond.

The structure of the TPR domain of the protein phosphatase PP5 reveals that each TPR motif of this domain consists of a pair of antiparallel α -helices of equivalent length, helix A and helix B (24). Adjacent TPR motifs are packed together in a parallel arrangement such that a tandem TPR motif structure is composed of a regular series of antiparallel α -helix: each α -helix shares two immediate α -helix neighbors and the protein fold may be defined as an overlapping array of three-helix bundles (24). Since a small residue at position 8 is located at the position of closest contact between the A and B α -helices of a TPR (24), substitution of the residue for the bulky residue Gln may lead to incorrect packing of the helix. This prediction is supported by a mutation of the p67^{phox} gene in a patient with CGD: the mutant protein with substitution of position 8 in the third TPR (Gly-78) for Glu appears unstable in phagocytes (47), probably due to misfolding of the TPR. In addition, mutations at this position within TPRs 5 and 7 of *cdc23* result in defect of protein function (49). Position 20 on helix B also resides between both helices A and B, while position 27 is located at the interface of three helices (A, B, and A') within a three-helix bundle (24). This bundle may be incorrectly packed by one amino acid deletion in the region of residues 21–26 within helix B. Both types of mutations (substitution of Gln for a residue at position 8 and deletion of a residue at position 22) in the first to third TPRs of p67^{phox} result in defective interaction with Rac (Fig. 5). Thus the three TPRs are folded such that the TPR domain interacts with Rac. The conclusion can explain how CGD is caused by three reported mutations within the first to third TPRs of p67^{phox}: deletion of three amino acid residues (Lys-19, Lys-20, and Asp-21) in the first TPR (50), deletion of Lys-58 in the second TPR (48) and substitution for Gly-78 in the third TPR (47), the latter two of which are reported to result in decreased amounts of the proteins in neutrophils (47, 48).

Arg-102, on the other hand, resides at position 32 of the third TPR. Since the position is located at the C terminus of helix B (24), Arg-102 is not likely involved in the packing of the TPR helices. This is supported by the finding that the protein carrying the R102E substitution appears to be as stable as the wild-type p67^{phox} *in vivo* (Fig. 10), and confirmed by the observations that substitution resulted in little change in both CD (data not shown) and ¹H NMR spectra (Fig. 8). This mutation thus does not affect the structural integrity of p67^{phox}. The basic residue is rather considered to constitute a binding inter-

face for Rac. Substitution of the basic residue Lys for Arg-102 slightly reduces the capability of binding to Rac, while replacement by a neutral or acidic residue leads to little or no interaction with Rac, respectively. Thus Arg-102 plays a crucial role in binding to Rac, probably via an ionic interaction. This may explain that replacement of Asp-38 in the effector loop of Rac by a neutral or basic residue abrogates binding to p67^{phox} (Fig. 1B; and Refs. 22 and 27). Taken together with the present experiments using mutant proteins, the binding to Rac requires a specific block of the TPRs of p67^{phox}, the first three motifs, containing Arg-102 as an interacting residue.

The TPRs of p67^{phox} by themselves, however, do not seem sufficient for the interaction, since the protein fragment comprising the first three or all TPRs (p67 (1–122) or p67 (1–167), respectively) was incapable of binding to Rac2 (Fig. 1). A region outside of the TPRs may be required for the structural integrity of the TPR domain and/or for stable interaction between p67^{phox} and Rac. A recent report has shown that p67^{phox} amino acid residues 170–199 can bind to Rac, but to a much lesser extent (51). It can be excluded that the TPR motifs do not physically interact with Rac but provide the structural framework to present residues 170–199 effectively to Rac, because Arg-102 in the third TPR appears to directly bind to Rac: p67 (1–242, R102E), containing both residues 170–199 and TPRs with a mutation unaffected the structural integrity, is incapable of binding to Rac (Fig. 7). There may be two (or more) sites of p67^{phox} that directly interact with Rac, both of which are required for stable interaction and activation of the NADPH oxidase. The protein that contains residues 170–199 but lacks the first three or all TPR motifs (p67 (126–242) or p67 (170–242), respectively) is not capable of activating the oxidase at all, as shown in this study (Fig. 6B).

Interaction of Rac with p67^{phox} has been considered to be required for activation of the phagocyte NADPH oxidase, based on the observations that mutant forms of Rac, defective in the interaction, are incapable of activating the enzyme *in vitro* (22, 25–27). The requirement, however, has not been evidenced by experiments using mutant forms of the target protein p67^{phox}, except a report showing that a protein containing deletion of Lys-58, being unstable, neither binds to Rac nor activates the oxidase (48). The present study demonstrates that a series of TPR mutants of p67^{phox}, defective in Rac binding, were all devoid of activity in the cell-free activation system of the oxidase (Fig. 6C). Among mutant proteins of p67^{phox} carrying substitution for Arg-102, the Rac binding activity correlates well with the capability of activating the oxidase *in vitro* (the wild-type > R102K > R102Q > R102E) (Fig. 9). Furthermore, the protein with the R102E substitution, leading to a complete loss of interaction with Rac, is also inactive in the whole cell activation system of the oxidase (Fig. 10). These observations provide strong evidence that the binding of Rac to p67^{phox} plays an essential role in activation of the NADPH oxidase both *in vivo* and *in vitro*.

On the other hand, the interaction between Rac and p67^{phox} is not sufficient for activating the NADPH oxidase. The correctly packed fourth TPR of p67^{phox}, in contrast to the other TPRs, does not seem involved in the interaction (Fig. 5), but is required for activation of the NADPH oxidase (Fig. 6C). The fourth TPR may be packed independently of the N-terminal three TPRs; it is rather conformed together with other regions, presumably forming an interface to interact with other oxidase factors, p47^{phox} or a cytochrome *b*₅₅₈ subunit (gp91^{phox} or p22^{phox}). In this context, it should be noted that about 10 residues C-terminal to the Rac-binding domain of p67^{phox} (residues 203–212) are also required for the oxidase activation (52, 53). It has been shown that, in some proteins harboring mul-

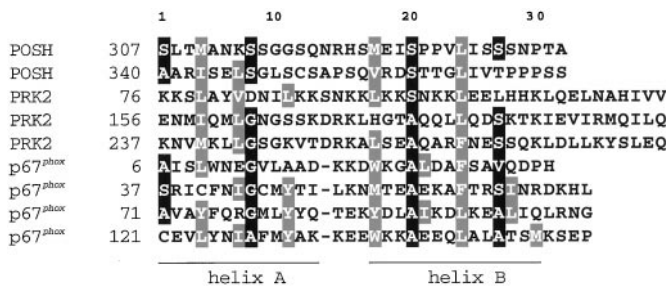


FIG. 11. Sequence alignment of the Rac-binding regions of POSH, PRK2, and p67^{phox}. Small and large hydrophobic residues are shown with black and shaded boxes, respectively. For details, see "Discussion."

multiple copies of TPR motifs, specific blocks of TPR motifs mediate interactions with particular target proteins and are assigned to specific biological functions. The N-terminal three TPR motifs of Ssn6p associate with the co-repressor Tup1p, whereas other combinations of TPR motifs mediate interactions with different transcription factors, which accounts for the diverse gene expression patterns regulated by Ssn6p (42, 54). TPR motifs 5–7 of p58, an inhibitor of the RNA-dependent protein kinase PKR, are responsible for interactions with PKR, while the N-terminal TPR motifs direct homotypic interactions (55).

Activation of the phagocyte NADPH oxidase is under strict control, since active oxygen species derived from superoxide are toxic to not only invading pathogens but also host cells, and thus unregulated production of superoxide results in damage of surrounding tissues accordingly. Since three indispensable proteins for the oxidase activation, p47^{phox}, p67^{phox}, and Rac, are all inactive in resting cells, each protein must be individually activated for superoxide production (10, 12, 16). In addition to these proteins, cell-free activation of the oxidase requires GTP (17–19) and anionic amphiphiles such as arachidonic acid (56): GTP binds to Rac, converting it to the active form, while arachidonic acid functions as an activator to induce conformational changes of both p47^{phox} and p67^{phox} (12, 15, 16). It has been reported that the TPR domain of protein phosphatase 5 is responsible for stimulation of the phosphatase activity by polyunsaturated fatty acids such as arachidonic acid (33, 34). It is tempting to postulate that arachidonic acid also interacts with the TPR domain of p67^{phox}, inducing a conformational change that culminates in oxidase activation.

Although the TPR domain of p67^{phox} is involved in the interaction with Rac as shown here, it is presently unknown whether the GTPase can bind to other TPR domains or not. The Rac-binding region of POSH, a novel adaptor protein harboring four SH3 domains, does not have a CRIB motif (57), but appears to contain repeated fragments reminiscent of TPR motifs or related sequences (Fig. 11), in which one additional amino acid residue is inserted between helices A and B when aligned with TPRs. It has recently been shown that PRK2, a protein kinase being considered as a target of Rho, can also interact with Rac (58). Its Rac-binding site appears to reside in the HR1 region that contains three leucine zipper-like sequences (59). In regions overlapping the sequences, small and large hydrophobic residues locate periodically as in TPR, but with one extra residue between helices A and B (Fig. 11). Thus such repeated helical structures as TPR domain would give a common architecture to conform a Rac-binding site. Future studies should be directed to the determination of structures of Rac target proteins complexed with the GTPase.

Acknowledgments—We are grateful to Drs. Takashi Ito (University of Tokyo) and Dongchon Kang (Kyushu University) for helpful discussions and encouragement, Dr. Y. Sugimoto (Japanese Foundation for Cancer Research) for advice on the retroviral vector system pSXL/C

pHa. We also thank Dr. Futoshi Kuribayashi (Kyushu University) for technical advice, and Y. Kage (Kyushu University), E. Ebisui (Tokyo Metropolitan Institute of Medical Science), and Drs. M. Iwata (Kumamoto University) and M. Y. Park (University of Tokyo) for technical assistance.

REFERENCES

- Van Aelst, L., and D'Souza-Schorey, C. (1997) *Genes Dev.* **11**, 2295–2322
- Hall, A. (1998) *Science* **279**, 509–514
- Manser, E., Leung, T., Salihuddin, H., Zhao, Z.-S., and Lim, L. (1994) *Nature* **367**, 40–46
- Burbelo, P. D., Drechsel, D., and Hall, A. (1995) *J. Biol. Chem.* **270**, 29071–29074
- Chanock, S. J., El Benna, J., Smith, R. M., and Babior, B. M. (1994) *J. Biol. Chem.* **269**, 24519–24522
- Jones, O. T. G. (1994) *BioEssays* **16**, 919–923
- Thrasher, A. J., Keep, N. H., Wientjes, F., and Segal, A. W. (1994) *Biochim. Biophys. Acta* **1227**, 1–24
- Roos, D., de Boer, M., Kuribayashi, F., Meischl, C., Weening, R. S., Segal, A. W., Ahlin, A., Nemet, K., Hossle, J. P., Bernatowska-Matuszkiewicz, E., and Middleton-Price, H. (1996) *Blood* **87**, 1663–1681
- DeLeo, F. R., and Quinn, M. T. (1996) *J. Leukocyte Biol.* **60**, 677–691
- Sumimoto, H., Ito, T., Hata, K., Mizuki, K., Nakamura, R., Kage, Y., Sakaki, Y., Nakamura, M., and Takeshige, K. (1997) In *Membrane Proteins: Structure, Function and Expression Control* (Hamasaki, N., and Mihara, K., eds) pp. 235–245, Kyushu University Press, Fukuoka, Japan
- Finan, P., Shimizu, Y., Gout, I., Hsuan, J., Truong, O., Butcher, C., Bennett, P., Waterfield, M. D., and Kellie, S. (1994) *J. Biol. Chem.* **269**, 13752–13755
- Sumimoto, H., Kage, Y., Nunoi, H., Sasaki, H., Nose, T., Fukumaki, Y., Ohno, M., Minakami, S., and Takeshige, K. (1994) *Proc. Natl. Acad. Sci. U. S. A.* **91**, 5345–5349
- Leto, T. L., Adams, A. G., and de Mendez, I. (1994) *Proc. Natl. Acad. Sci. U. S. A.* **91**, 10650–10654
- Ito, T., Nakamura, R., Sumimoto, H., Takeshige, K., and Sakaki, Y. (1996) *FEBS Lett.* **385**, 229–232
- Sumimoto, H., Hata, K., Mizuki, K., Ito, T., Kage, Y., Sakaki, Y., Fukumaki, Y., Nakamura, M., and Takeshige, K. (1996) *J. Biol. Chem.* **271**, 22152–22158
- Hata, K., Ito, T., Takeshige, K., and Sumimoto, H. (1998) *J. Biol. Chem.* **273**, 4232–4236
- Abo, A., Pick, E., Hall, A., Totty, N., Teahan, C. G., and Segal, A. W. (1991) *Nature* **353**, 668–670
- Knaus, U. G., Heyworth, P. G., Kinsella, B. T., Curnutte, J. T., and Bokoch, G. M. (1992) *J. Biol. Chem.* **267**, 23575–23582
- Mizuno, T., Kaibuchi, K., Ando, S., Musha, T., Hiraoka, K., Takaiishi, K., Asada, M., Nunoi, H., Matsuda, I., and Takai, Y. (1992) *J. Biol. Chem.* **267**, 10215–10218
- Dorseuil, O., Vazquez, A., Lang, P., Bertoglio, J., Gacon, G., and Leca, G. (1992) *J. Biol. Chem.* **267**, 20540–20542
- Gabig, T. G., Crean, C. D., Mantel, P. L., and Rosli, R. (1995) *Blood* **85**, 804–811
- Diekmann, D., Abo, A., Johnston, C., Segal, A. W., and Hall, A. (1994) *Science* **265**, 531–533
- Ponting, C. P. (1996) *Protein Sci.* **5**, 2353–2357
- Das, A. K., Cohen, P. T. W., and Barford, D. (1998) *EMBO J.* **17**, 1192–1199
- Diekmann, D., Nobes, C. D., Burbelo, P. D., Abo, A., and Hall, A. (1995) *EMBO J.* **14**, 5297–5305
- Xu, X., Barry, D. C., Settleman, J., Schwartz, M. A., and Bokoch, G. M. (1994) *J. Biol. Chem.* **269**, 23569–23574
- Nisimoto, Y., Freeman, J. L. R., Motalebi, S. A., Hirshberg, M., and Lambeth, J. D. (1997) *J. Biol. Chem.* **272**, 18834–18841
- Hirano, T., Kinoshita, N., Morikawa, K., and Yanagida, M. (1990) *Cell* **60**, 319–328
- Sikorski, R. S., Boguski, M. S., Goebel, M., and Hieter, P. (1990) *Cell* **60**, 307–317
- King, R. W., Peters, J.-M., Tugendreich, S., Rolfe, M., Hieter, P., and Kirschner, M. W. (1995) *Cell* **81**, 279–288
- Goebel, M., and Yanagida, M. (1991) *Trends Biochem. Sci.* **16**, 173–177
- Kyrpidis, N. C., and Woese, C. R. (1998) *Trends Biochem. Sci.* **23**, 245–247
- Chen, M. X., and Cohen, P. T. W. (1997) *FEBS Lett.* **400**, 136–140
- Skinner, J., Sinclair, C., Romeo, C., Armstrong, D., Charbonneau, H., and Rossie, S. (1997) *J. Biol. Chem.* **272**, 22464–22471
- Dorseuil, O., Reibel, L., Bokoch, G. M., Camonis, J., and Gacon, G. (1996) *J. Biol. Chem.* **271**, 83–88
- Sugimoto, Y., Aksentjevich, I., Gottesman, M. M., and Pastan, I. (1994) *Bio/Technology* **12**, 694–698
- de Mendez, I., Adams, A. G., Sokolic, R. A., Malech, H. L., and Leto, T. L. (1996) *EMBO J.* **15**, 1211–1220
- Nakamura, M., Murakami, M., Koga, T., Tanaka, Y., and Minakami, S. (1987) *Blood* **69**, 1404–1408
- Iwata, M., Nunoi, H., Matsuda, I., Kanegasaki, S., Tsuruo, T., and Sugimoto, Y. (1998) *Hum. Genet.* **103**, 419–423
- Yang, J. T., Wu, C.-S. C., and Martinez, H. M. (1986) *Methods Enzymol.* **130**, 208–269
- Freeman, J. L. R., Kreck, M. L., Uhlinger, D. J., and Lambeth, J. D. (1994) *Biochemistry* **33**, 13431–13435
- Smith, R. L., Redd, M. J., and Johnson, A. D. (1995) *Genes Dev.* **9**, 2903–2910
- Tugendreich, S., Boguski, M. S., Seldin, M. S., and Hieter, P. (1993) *Proc. Natl. Acad. Sci. U. S. A.* **90**, 10031–10035
- Bömer, U., Pfanner, N., and Dietmeier, K. (1996) *FEBS Lett.* **382**, 153–158
- Kyte, J., and Doolittle, R. F. (1982) *J. Mol. Biol.* **157**, 105–132
- Mizuki, K., Kadomatsu, K., Hata, K., Ito, T., Fan, Q.-W., Kage, Y., Fukumaki, Y., Sakaki, Y., Takeshige, K., and Sumimoto, H. (1998) *Eur. J. Biochem.*

- 251, 573–582
47. de Boer, M., Hilarius-Stokman, P. M., Hossle, J.-P., Verhoeven, A. J., Graf, N., Kenney, R. T., Seger, R., and Roos, D. (1994) *Blood* **83**, 531–536
48. Leusen, J. H. W., de Klein, A., Hilarius, P. M., Ahlin, A., Palmblad, J., Smith, C. I. E., Diekmann, D., Hall, A., Verhoeven, A. J., and Roos, D. (1996) *J. Exp. Med.* **184**, 1243–1249
49. Sikorski, R. S., Michaud, W. A., and Hieter, P. (1993) *Mol. Cell. Biol.* **13**, 1212–1221
50. Patiño, P. J., Rae, J., Erickson, R., Ding, J., Garcia de Ollate, D., and Curnutte, J. T. (1996) *Blood* **88**, Suppl. 1, 622a
51. Ahmed, S., Prigmore, E., Govind, S., Veryard, C., Kozma, R., Wientjes, F. B., Segal, A. W., and Lim, L. (1998) *J. Biol. Chem.* **273**, 15693–15701
52. Hata, K., Takeshige, K., and Sumimoto, H. (1997) *Biochem. Biophys. Res. Commun.* **241**, 226–231
53. Han, C.-H., Freeman, J. L. R., Lee, T., Motalebi, S. A., and Lambeth, J. D. (1998) *J. Biol. Chem.* **273**, 16663–16668
54. Tzamarias, D., and Struhl, K. (1995) *Genes Dev.* **9**, 821–831
55. Gale, M., Jr., Tan, S.-L., Wambach, M., and Katze, M. G. (1996) *Mol. Cell. Biol.* **16**, 4172–4181
56. Bromberg, Y., and Pick, E. (1985) *J. Biol. Chem.* **260**, 13539–13545
57. Tapon, N., Nagata, K., Lamarche, N., and Hall, A. (1998) *EMBO J.* **17**, 1395–1404
58. Vincent, S., and Settleman, J. (1997) *Mol. Cell. Biol.* **17**, 2247–2256
59. Flynn, P., Mellor, H., Palmer, R., Panayotou, G., and Parker, P. J. (1998) *J. Biol. Chem.* **273**, 2698–2705